

Noise assisted high performance linear inductive distance sensor

Abstract. A temperature compensated linear inductive distance sensor assisted by added noise is demonstrated. The mixed signal processing algorithm performs an effective interpolation over a low-resolution two-dimensional calibration table addressed directly by the digitized noise-affected signals of distance and temperature sensing modules without further arithmetic operations. The table entries are directly passed to the output digital-to-analog converter. The output noise will be cancelled by the intrinsic low-pass behavior of the power output stage. The operation distance, the linearity parameters, as well as the performance of the sensor exceed the standard of the respective industrial products.

Streszczenie. W artykule opisano liniowy indukcyjny czujnik odległości z dodanym sygnałem szumu. Algorytm działający na sygnał mieszany wyznacza skuteczną interpolację dwuwymiarowej tablicy kalibracyjnej o niskiej rozdzielczości adresowanej bezpośrednio przez sygnały cyfrowe odległości i temperatury bez dalszych operacji arytmetycznych. Wejścia tablicowe są bezpośrednio kierowane na wyjście przetwornika cyfrowo-analogowego. Wyjściowy szum może być skasowany przez wewnętrzną nisko-pasmową pracę wyjścia mocy. Odległość działania, parametry liniowości, a także działanie czujnika przekraczają standardy odpowiednich produktów przemysłowych. (Działanie liniowego indukcyjnego czujnika odległości z sygnałem szumu).

Keywords: Distance measurement, inductive sensors, additive noise, linearization techniques, temperature dependence.

Słowa kluczowe: pomiar odległości, czujniki indukcyjne, szum dodany, techniki linearyzacyjne, zależność temperaturowa.

doi:10.12915/pe.2014.12.29

Introduction

Industry sets a high value on linear operation of inductive distance sensors [1] in a broad range of temperature. Sensors of this class consist of a primary sensing element, typically an inductor with open magnetic circuit, e.g. a ferrite pot core (Fig. 1), an oscillator circuit to excite the inductor as a part of an LC circuit, resulting in a periodic, nearly sinusoid signal, an amplitude, phase or frequency sensitive demodulator circuit, and an evaluation circuit to evaluate the measuring signal and generate sensor output.



Fig.1. Primary sensing element of an inductive sensor

The easy and precise calibration is also very important in the mass production of these sensors. The previous criteria can be efficiently fulfilled by a microprocessor controlled measurement and evaluation system which is an effective solution in the case of compact inductive distance sensors.

It would be quite straightforward to develop temperature independent high-resolution sensors by the application of high speed microcontrollers, high resolution analog to digital converters (ADC) and digital to analog converters (DAC), expensive and precise elements to record the measuring signal with a high precision and to calculate the temperature independent linear output of the sensor via the solution of e.g. polynomial equations and interpolations [2]. The drawbacks of these solutions are the low response time due to the high amount of calculations and the high price of the electronic components.

In this paper, a noise-enhanced [3] [4] measurement chain is presented, based on fast and reliable temperature compensation and linearization method using a low-cost, small footprint microcontroller, low-resolution, but high-speed A/D and D/A converters. The application of this solution results in a fast, low-cost, temperature independent, compact high-linearity inductive distance sensor.

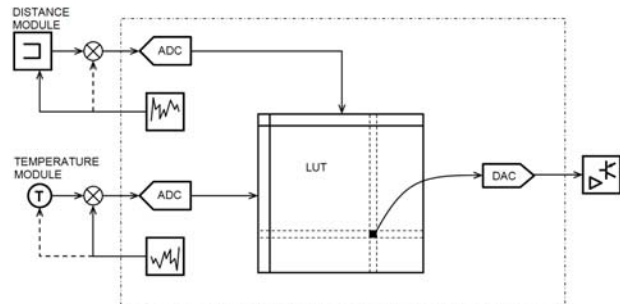


Fig.2. Schematic block diagram of the noise assisted distance sensor. The elements surrounded by dashed-dotted line can be realized by the means of a microcontroller. The distance module consists of an LC circuit, an oscillator and a demodulator. The temperature module provides a DC voltage as a function of the temperature.

Noise assisted measurement and evaluation chain

An 8 bit microcontroller has been completed by two relatively fast 8 bit A/D converters and an 8 bit D/A converter. The block diagram of the measurement and evaluation method is shown in Fig. 2.

The primary sensing element (parallel LC circuit with an inductor with ferrite pot core) is oscillated by a positive feedback circuit resulting in an essentially sinusoid voltage, and the demodulated voltage of the sensing element is measured by an A/D converter. In our case, the noise was coupled to the supply current of the oscillator making stochastically varying oscillation amplitude, but it is also practical to mix the noise component directly to the input of the A/D converter. In parallel, the voltage of a temperature sensing circuit (i.e. an NTC) with another superposed noise is quantized by another A/D converter.

It would be straightforward to apply a calibration table, e.g. a look-up table (LUT) for the generation of the temperature-independent linearized output via interpolation between the table entries indexed by (fractional) values of oscillation amplitude and temperature related digitized and averaged values. In contrast, in our treatment, the numerical interpolation is not necessary in the present system, because the interpolation will be efficiently performed by the noise superposed on the measurement signals. The interpolation of the calibrated output data via stochastic addressing of the calibration LUT is illustrated in Fig. 3.

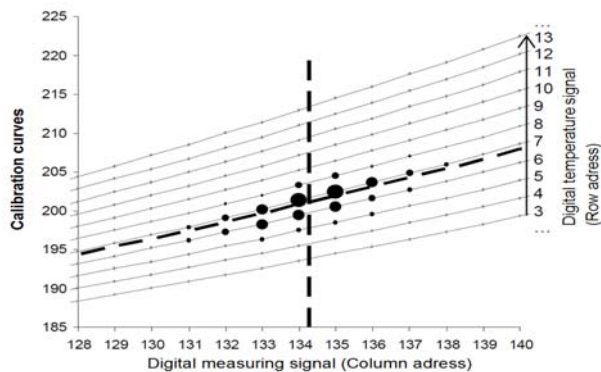


Fig.3. Visualization of the evaluation method based on the calibration curves. The different calibration curves belong to different ambient temperatures.

Assuming that the actual target distance and the temperature correspond to fractional values of the respective digital measurement signals represented by the dashed lines, both column address and row address possess specific distributions around these values due to added noise. Further, assuming that the two noise components are not correlated, the addressed calibrated values scatter around the theoretical calibrated value corresponding to the precise target distance and temperature, as marked by the crossing point of the dashed lines.

The probability of occurrence of the digital values around the average value is represented by the size of the spots in the figure. The stochastically addressed calibrated output values are directly converted to analog signal and passed to the power output stage, where an effective low-pass filtering takes place due to the intrinsic low-pass character of the typical power amplifiers. As an alternative to the analog sensor output, the calibrated output values may undergo a digital filtering, and the filtered data can be uploaded to an IO module of a sensor network [5]. N.B. a digital communication interface will be normally needed for the measurement of typical temperature dependent sensor characteristics and for recording individual sensor characteristics to be used for piecewise linearization or calibration.

Application example

The distance module was constructed with a coil with ferrite pot core corresponds to an M18 size inductive sensor, which is one of the popular formats of industrial inductive sensors. A pre-recorded quasi-random bit sequence is read out from the flash memory and is put to a specified pin of the microcontroller. It was also tested to use the least significant bit of the latest conversion value as binary noise. The filtered digital demodulated voltage data was recorded for different sensor to target distances and different stabilized temperatures, though in the presence of added noise at the input of the respective ADCs, but with digital filtering (Fig. 4).

In order to generate the LUT elements, the physical distance as a function of filtered digital demodulated voltage and filtered temperature signal was first extrapolated to low and high temperatures beyond the real operation temperature range, to cover all possible values of the digitized distance and temperature related voltages, and finally scaled and truncated to the nearest integer to fit to the input of the output DAC. This LUT (Fig. 5) is treated as inverse characteristics or calibration data to be downloaded into the flash memory of the microcontroller of the sensor.

In our example, the linearity range of the sensor was considered between 0 and 6 mm, according to the DAC output span of 0 to 2.7 V. The measured characteristics of

the system depicted in Fig. 1 as a linearized and temperature compensated sensor is shown in Fig. 6, for a wide range of temperatures. Please note that these actual temperature values were neither applied during recording of the measurement data in Fig. 4, nor necessarily directly represented in the LUT in Fig. 5.

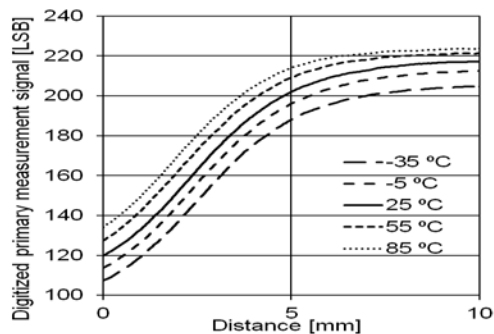


Fig.4. The filtered demodulated voltage characteristics of the distance module for different temperatures. B. The visualized calibration table.

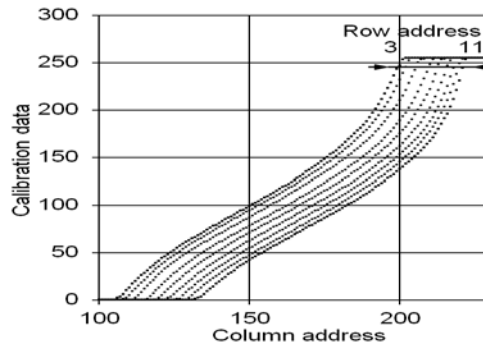


Fig.5. The visualized calibration table.

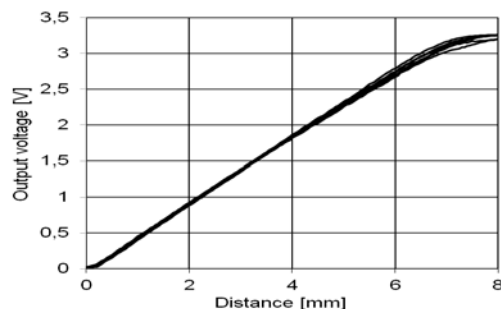


Fig. 6. Temperature independent, linear output data of the sensor. The curves belong to the following ambient temperatures: -30°C, -10°C, 0°C, 20°C, 40°C, 60°C, 80°C.

The error of the output was calculated as the difference between the real output voltage and the expected voltage corresponding to the actual sensor to target distance (Fig. 7). For any temperatures, the linear sensing range, output error, temperature drift and linearity error figures are definitely better than those of the analogous commercially available devices in the M18 size class.

The actual update rate of the output is 55 kHz. For any desired sensor performance the oversampling frequency and the intrinsic low-pass filtering characteristics of the power output stage should be specified according to the trade-off between the output noise and the modulation bandwidth of the complete sensor [6].

Upon the mass production of sensors two problems will arise. First, due to manufacturing deviations and the parameter deviations of the electronic components, the produced individual pieces can slightly differ in the temperature characteristics. As second, the recording of the temperature dependent behavior of individual sensors is not possible because of the required time. However, these

types of sensors possess typical temperature behavior, thus the demodulated voltage versus target distance characteristics measured at the manufacturing temperature can be extrapolated to the complete operation temperature range with very high reliability. The individual calibration data can be generated from this semi-empirical data set.

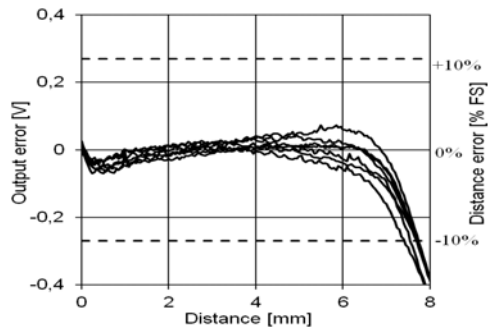


Fig. 7. Error of the sensor. The curves belong to the following ambient temperatures: -30°C, -10°C, 0°C, 20°C, 40°C, 60°C, 80°C.

Discussion

The performance of the output of an inductive distance sensor can be well characterized by the signal-to-noise ratio (SNR) of the output signal. The output signal is practically the output voltage – or alternatively the output data in digital form – which is theoretically the linear function of the of the sensor-to-target distance. The standard deviance of the output error is considered to be the noise, regardless whether it is a quantization error or coming from another source. The signal-to-noise ratio will be defined as the reciprocal of the standard deviance,

$$(1) \quad SNR = \frac{1}{\sqrt{\sum_{i=0}^{n-1} \frac{(x_i - \mu)^2}{n}}}$$

where x_i is the value of the i -th sample, μ is the expected output data and n is the number of the samples.

In order to analyze the signal-to-noise ratio with and without noise added to the primary measurement signals for various ADC and DAC resolutions and output filter characteristics, a theoretical mathematical model was implemented in LabView environment.

The model generates the target distance dependent measurement signal as primary sensing signal. A low-pass filtered random bit generator signal is added to the primary distance sensing signal, and the sum is digitized by an analog-to-digital converter model. The ADC is followed by a look-up table; it should be noted here that for the sake of clarity the simulation model does not consider the temperature dependence and the look-up table is addressed by the noise-perturbed digitized distance dependent data only. The stochastically addressed values of the lookup table are passed to a digital-to-analog converter mode, and finally the output of the DAC is filtered by a low-pass filter. The resolution of the ADC and DAC, as well as the cut-off frequency of the output filter are selectable arbitrarily.

At first, the output characteristics of the linearized sensor model were recorded for the noise-free case. In Fig. 8 the output signal is shown in the function of the sensor-to-target distance and the error of the output is also presented.

The resolution of the ADC was 8 bits, which was effectively further reduced by the fact that, due the assumed characteristics of the primary sensing elements, the digitized values were between 104 and 164, i.e. less than a quarter of the ADC input range was used. The quantization error can be observed easily in the throughout the whole sensing range. The error of the output increases rapidly

with the sensor-to-target distance and around the end of the sensing range it exceeds the 3 percent.

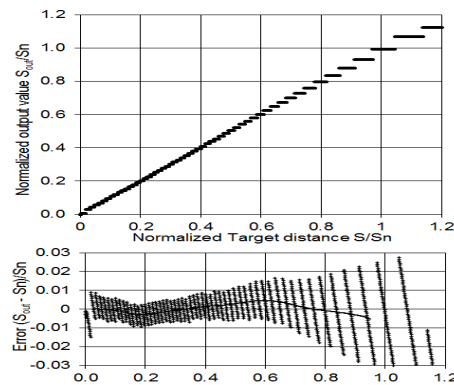


Fig. 8. Simulated output characteristics and output error of the sensor model without additional input noise.

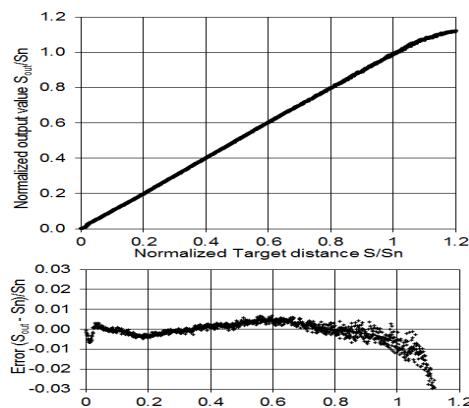


Fig. 9. Simulated output characteristics and output error of the sensor model without additional input noise.

By adding optimal amount of noise to the measurement signal (i.e. the input of the ADC) the linearity of the output is improved significantly, thus the output error remains at a low level, as it shown in Fig. 9. It is observable that the nonlinearity caused by the quantization error improved effectively even for larger sensor-to-target distances. At the end of the sensing range the output error just exceeds the 1 percent, below that it remains much lower. Upon further increase of the noise amplitude above the optimal level, the output signal becomes noisier, as it can be expected, thus the error increases again.

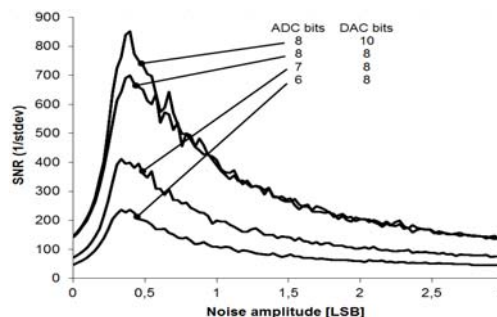


Fig. 10. Signal-to-noise ratios of the sensor output characteristics as the function of the noise amplitude for different ADC and DAC resolutions. The graph shows simulations results.

We examined the SNR of the system for different ADC and DAC resolutions and for different amplitudes of the added noise (Fig. 10). The signal-to-noise ratio has a maximum value at the certain amplitude of the additional noise signal in every cases. The highest SNR amplification was experienced in the case of 8 bits ADC and 10 bits DAC whereas the signal-to-noise ratio was 5.8 times higher with

additional noise than without. It can be definitely concluded that the low signal-to-noise ratio in the noise-free cases is caused by the quantization error of the analog-to-digital converter.

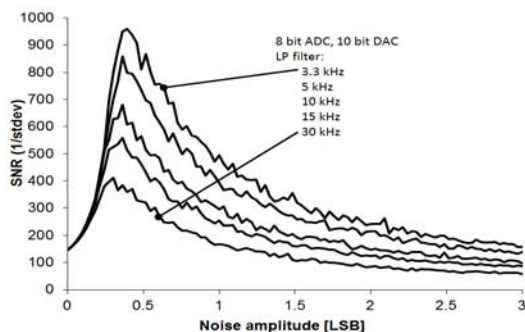


Fig. 11. Signal-to-noise ratios of the sensor output characteristics as the function of the cut-off frequency of the output low-pass filter. The graph shows simulations results.

The maximum of the SNR was found around the noise amplitude of 0.45 LSB in every case, expressed in units of the amplitude according to the least significant bit of the respective ADC. For higher noise amplitudes the SNR curve decays, because the output filter is no longer able to remove the stochastic fluctuations from the signal effectively.

The SNR characteristics of the sensor output were also calculated as the function of the cut-off frequency of the output low-pass filter characteristics (Fig. 11). The maxima of the individual curves were observed between 0.4-0.5 LSB noise amplitude. Higher signal-to-noise ratio amplification was reached with lower low-pass filter cut-off frequencies, i.e. effective filtering improves the maximum achievable signal-to-noise ratio. The tuning of the output filter characteristics in a real sensor application is a trade-off between the output speed and the precision of the output signal.

In mixed signal systems the dithering is a well-known technique for example for decreasing the quantization error or the increasing of the linearity of analog-to-digital converters by adding noise to the input signal [7]. Since the characteristic of real analog-to-digital converters is never optimal, deterministic, repeated and correlated error is produced by the imperfect quantization or re-quantization of analog or digital information which causes distortions in the resulting output signal. Due to the random fluctuations added to the input of the device, the previously mathematically determinable output errors become stochastic, therefore the distortion of the output signal decreases.

Our case is, however, distinct from the dithering technique, where the parameters (resolution, linearity etc.) of an analog-to-digital converter are improved by means of noise added to the input, oversampling and digital filtering of the numerical output value. Dithering itself is related to the A/D-conversion only.

In our treatment, the intentionally added noise remains in the system even after digitization and during the further processing until the output filter, and the resulted system is a linearized and temperature independent distance sensor.

The system comprising the sensing elements of distance and temperature, the noise generators and mixers, the A/D-converters of the noise-affected sensing signals, the look-up table and the subsequent D/A-converter has a limited number of states due to the limited number and word length of the look-up table entries. However, due to the added noise, the output of the complete system is faithfully

representing the input excitation, i.e. the distance of the target from the sensor. The SNR curves shown in Figs. 10 and 11 possess well-defined maxima for a given non-zero noise amplitude, which makes our solution a subject of stochastic resonance [8].

Conclusions

A linearized, temperature compensated inductive distance sensor assisted by additional noise was demonstrated. The mixed signal processing algorithm performs an effective interpolation over a low resolution two dimensional table addressed by noise affected A/D converted signals of distance and temperature sensing modules without further arithmetic operations. The operation distance, the linearity parameters and the performance of the sensor all exceed the standard of the respective industrial products.

It was shown that the signal-to-noise ratio of the system has a maximum at the certain level of the added noise amplitude which feature is typical of the phenomenon stochastic resonance.

Zoltán Pólik is indebted for the support by the European Union and the State of Hungary, co-financed by the European Social Fund in the framework of TÁMOP 4.2.4. A/2-11-1-2012-0001 'National Excellence Program'.

REFERENCES

- [1] Fericean S., Droxler R., New Noncontacting inductive analog proximity and inductive linear displacement sensors for industrial automation, *IEEE Sensors Journal*, Vol. 7 (2007), No. 11, 1538-1545.
- [2] Žorić A. C., Martinović D., Obradović S., A Simple 2D Digital Calibration Routine for Transducers, *Facta universitatis - series: Electronics and Energetics*, Vol. 19 (2006), No. 2, University of Niš, 197-207.
- [3] Luchinsky D. G., Mannella R., McClintock P. V. E., Stocks N. G., Stochastic Resonance in Electrical Circuits-I: Conventional Stochastic Resonance, *IEEE Transactions on Circuits and Systems-II: Analog and digital signal processing*, Vol. 46 (1999), No. 9., 1205-1214.
- [4] Gammaitoni L., Stochastic resonance and the dithering effect in threshold physical systems, *Physical review E*, Vol. 52 (1995), No. 5, 4691-4699.
- [5] Kása Z., Decentralized IO Solutions in the industrial automation, *Proceedings of Factory Automation 2013*, University of Pannonia, Veszprem, Hungary (2013), 49-54.
- [6] Makra P., Topalian Z., Granqvist C. G., Kish L. B., Kwan C., Accuracy versus speed in fluctuation-enhanced sensing, *Fluctuation and Noise Letters*, Vol. 11 (2012), No. 2.
- [7] Lal-Jadziak J., Sienkowski S., Cross-correlation Function Determination by Using Deterministic and Randomized Quantization, *Przegląd Elektrotechniczny*, Vol. 89 (2013), No. 1a, 81-83.
- [8] Gingl Z., Kiss L. B., Moss F., Non-Dynamical Stochastic Resonance: Theory and Experiments with White and Arbitrarily Coloured Noise, *Europhysics Letters*, Vol. 29 (1995), No. 3, 191-196.

Authors: Dr. Zoltán Kántor, PhD in Physics in 1997. Materials research and laser processing of solids as senior research fellow at the Research Group on Laser Physics of the Hungarian Academy of Sciences. Associate professor of the Institute of Physics and Mechatronics of the University of Pannonia. Team manager of Corporate Innovation Management, Balluff Elektronika Kft., Veszprém, Hungary., E-mail: zoltan.kantor@balluff.hu; Zoltán Pólik, M.Sc. in Electrical Engineering in 2011. Ph.D. student at the Széchenyi István University of Győr. Research and development engineer in the team Corporate Innovation Management at the Balluff Elektronika Kft., Veszprém, Hungary. E-mail: zoltan.polik@balluff.hu.